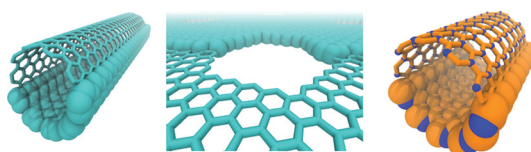


# What Have We Learnt About the Mechanisms of Rapid Water Transport, Ion Rejection and Selectivity in Nanopores from Molecular Simulation?

Michael Thomas, Ben Corry,\* and Tamsyn A. Hilder\*



## From the Contents

1. Introduction .....	1454
2. Types of Nanopores .....	1454
3. Modeling Approaches.....	1455
4. Reports of Rapid Transport and Selectivity in Nanopores.....	1455
5. Mechanisms Involved in Transport/ Selectivity.....	1458
6. Modeling Limitations.....	1462
7. Applications .....	1462
8. Conclusion .....	1463

**N**anopores have demonstrated an extraordinary ability to allow water molecules to pass through their interiors at rates far exceeding expectations based on continuum theory. Moreover, simulation studies suggest that particular nanoscale pores have the potential to discriminate between water and salts as well as to distinguish between a range of different ion types. Some of the unusual features of transport in these nanopores have been elucidated with molecular dynamics simulation, specifically the spontaneous filling and rapid transport of water, the rejection of ions and the selection between ions. The main focus of this review, however, is the physical mechanisms which act to produce such remarkable behaviour at this scale, drawing on the many studies that have been conducted in the last decade. Since molecular dynamics simulations allow the motion of individual atoms to be followed over time, they have the potential to provide fundamental insight into the reasons why transport in nanoscale pores differs from expectations based on macroscopic theory. Gaining an understanding of the mechanisms of transport in these tiny pores should guide future experiments in this area aimed at developing novel technologies and improving existing membrane separation techniques.

## 1. Introduction

Carbon nanotubes and other nanostructured porous materials have received a lot of attention in recent years due to their remarkable optical, electronic, thermal and mechanical properties. As a consequence, these materials have been suggested for use in an enormous range of applications including the desalination of sea water;<sup>[1–3]</sup> the removal of dangerous contaminants from water supplies;<sup>[4,5]</sup> the separation of gases, ions and biomolecules;<sup>[6–8]</sup> the sequencing of DNA;<sup>[9]</sup> electrical devices and biosensors;<sup>[10,11]</sup> and nanofluidic devices.<sup>[12]</sup> Many of these applications involve flowing liquids or gases through the interior of the pores. Surprisingly little is known about the fundamental behaviour of molecules transporting through nanotubes and graphene despite the potential materials and devices which may be constructed from these tiny channels.

Computer modelling is at the forefront of nanotube-based device design, guiding the experimental processes needed to produce benefits to the wider community. Nanopores display a range of unusual transport and selectivity properties, in both simulations and experiment. One of the motivations for conducting quantum mechanics calculations and classical molecular dynamics simulations is to allow the physical mechanisms underlying this behaviour to be elucidated. This review will focus on the computational study of transport and selectivity of nanopores, as well as the contribution of computational modelling toward our understanding of the unique mechanisms involved.

In this review we aim to summarise what has been learnt from molecular dynamics simulations about the physical reasons that nanopores display unusual transport properties. In particular we hope to help elucidate:

- Why water fills the interior of hydrophobic and hydrophilic nanopores
- Why the transport of water and other molecules through some nanopores is so fast
- How nanopores are able to reject salts while passing water
- How nanopores can select between different ion types

There have been several recent reviews which have briefly described progress on the use of molecular simulations to purify water using nanoporous carbon membranes<sup>[13,14]</sup> and to create ion selective pores.<sup>[15]</sup> In contrast, here we focus on what has been learnt from simulations about the mechanisms of transport.

## 2. Types of Nanopores

### 2.1. Nanotubes

Over the last few decades a range of nanopores have been synthesised. Perhaps the most well known are carbon nanotubes which are cylindrical structures composed of one or more layers of carbon (**Figure 1A**). Such nanotubes have internal pore diameters as small as 1.0 nm<sup>[16]</sup> to many tens of nm.<sup>[17]</sup> As most nanotubes are capped at the ends, they have to be ‘opened’ to allow transport to occur in their interior.

For the measurement of transport through nanotubes, this has been done most effectively by forming membranes containing aligned carbon nanotubes and chemically etching the surfaces to open the pores.<sup>[18,19]</sup>

Since they are comprised of pure carbon, the atoms comprising the majority of the nanotube are usually believed to carry no partial charge yielding a non-polar hydrophobic surface. However, it was shown using quantum mechanical calculations that partial charges on the carbon atoms near the opening of the nanotubes deviated significantly from zero, while the remainder were approximately zero.<sup>[20]</sup> In addition, water molecules have been demonstrated to induce charges on carbon nanotube atoms.<sup>[21]</sup> Furthermore, many carbon nanotubes are likely to contain defects such as holes or other elements,<sup>[22–24]</sup> and the etching required to open the nanotubes usually functionalises the ends of the nanotubes with carboxylic, carbonyl and hydroxyl groups,<sup>[25]</sup> all of which will change the electronic nature of the pore and must be considered when trying to explain transport properties.

Nanotubes can also be fabricated from materials alternate to carbon, for example boron nitride (**Figure 1C**), and silicon carbide.<sup>[26]</sup> Boron nitride nanotubes were first synthesized by Chopra et al.<sup>[27]</sup> who obtained multi-walled tubes with inner diameters in the order of 1–3 nm. Silicon carbide nanotubes have been synthesized with diameters ranging from 10–100 nm depending on synthesis method used.<sup>[28,29]</sup> These nanotubes exhibit a hexagonal array of alternating atoms, each of which can be expected to carry either a positive or negative charge creating a polar pore interior due to the unequal electronegativity of boron and nitrogen, or silicon and carbon.<sup>[30–32]</sup> Boron nitride and silicon carbide nanotubes have been shown to buckle as a result of these differences in electronegativity.<sup>[33–35]</sup>

The pore size and chirality of nanotubes are often defined by their chiral vector, (n,m), as explained in<sup>[36]</sup> and many other publications. This results in three general forms: arm-chair (n,n), chiral (n,m) and zigzag (n,0) nanotubes, where larger values of n and m refer to wider pores.

### 2.2. Graphene

Just as nanotubes can be constructed with differing pore radii and atomic composition, they can also have different lengths. But perhaps the simplest way to construct an extremely short pore is to form holes in graphene (**Figure 1B**). Graphene is a material which is composed of carbon atoms arranged in a hexagonal array and is only one-atom thick. Graphene sheets generally contain defects, either as atoms of other elements being incorporated into the sheet or as holes. Size selective

Dr. M. Thomas, Dr. B. Corry, Dr. T. A. Hilder  
Research School of Biology  
Australian National University  
ACT 0200, Australia  
E-mail: ben.corry@anu.edu.au;  
tamsyn.hilder@anu.edu.au



DOI: 10.1002/sml.201302968

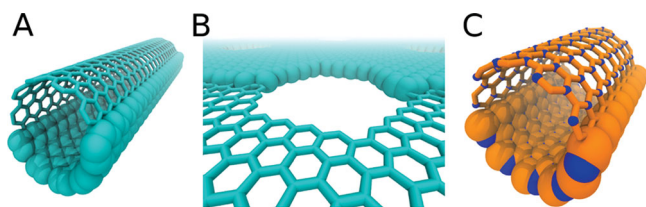


**Figure 1.** Cutaway representations of (A) A 5 nm long, (10, 10) carbon nanotube. (B) A nanopore in a graphene sheet. (C) A 2 nm long, (10, 10) boron nitride nanotube. Carbon is represented in cyan, nitrogen in blue and boron in orange. In each case half the atoms are shown as sticks and half in space filling representation.

transport of molecules through graphene has recently been reported and explained as arising through intrinsic pore defects 1–15 nm in size.<sup>[37]</sup>

Nanopores can be intentionally introduced into the graphene structure by chemical or plasma etching, or via exposure to ion or electron beams. Features as small as 100 nm can be made by masking and etching the surface.<sup>[38–40]</sup> The inclusion of pores or functional groups down to 5 nm in size have been obtained via selective lithographic functionalization.<sup>[41,42]</sup> Pores as small as 20 nm diameter have been produced using focussed ion beams<sup>[43,44]</sup> while more remarkably, controlled pores of sizes as small as 3 Å radius (corresponding to the removal of 10 atoms) have been obtained experimentally via ion and electron bombardment of graphene sheets.<sup>[45]</sup> The ability to create pores of various sizes in graphene sheets and to alter the chemical functionality on the pore rims may have the potential to yield a range of one-atom thick pores with different transport properties.

### 3. Modeling Approaches

Molecular dynamics (MD) is an important tool for researchers investigating the transport of small molecules through nanopores as the atomic resolution of MD simulations allows for the investigation of many important features of transport over timescales long enough to collect adequate statistics. It allows researchers to capture many permeation events of single ions and water molecules through nanopores and to calculate the energetics of ion and water permeation. Although this review focuses on molecular dynamics, many studies have been conducted for water in nanotubes using Monte Carlo simulations.<sup>[46–48]</sup> The results from these studies can complement MD even though they may not allow the direct observation of the mechanisms of transport.

In MD, the motion of all the atoms in the system is followed over time with the interactions between atoms described by empirical potentials. These trajectories of the atoms can then be analysed to determine structural and dynamic properties of the system as well as to derive quantities such as free energies, mean square displacements and other correlation functions. Unfortunately, although more accurate than MD, quantum mechanical (QM) simulations are more computationally demanding, therefore it is presently not possible to run QM calculations long enough to directly measure transport. However, QM is still often

employed in the study of nanopores to either determine static properties or to generate parameters for the empirical potentials used in MD as often these parameters are not yet available in the literature. Providing details of these methods is beyond the scope of this review; for further details of the method the reader is referred to Ebro et al.<sup>[14]</sup>

In initial investigations, Hummer et al. modelled carbon nanotubes in bulk water in order to investigate their water filling and transport properties.<sup>[49]</sup> But, to study transport through nanopores under a driving force in MD simulations, nanopores typically need to be arranged so as to form a continuous sheet or membrane that can separate two reservoirs. It is possible that the way in which this is done will influence the simulated transport rates and mechanisms. Forming a membrane is straight forward for graphene, but for nanotubes they are typically embedded in some form of impermeable matrix through which the nanotubes create pores. In experiments, nanotubes are often embedded in silicon nitride<sup>[1]</sup> or a polystyrene film.<sup>[18,50]</sup> In MD simulations, nanotubes have been embedded in a variety of matrices including silicon nitride,<sup>[51]</sup> lipid bilayers,<sup>[52]</sup> and graphene bilayers,<sup>[53,54]</sup> as shown in **Figure 2**. An alternative approach, developed by Zhu and Schulten,<sup>[55]</sup> involves packing the nanotubes close together such that there is not enough space for molecules to pass between them and a matrix is not required (Figure 2D). This setup is popular as it allows fluxes to be measured across many nanotubes instead of just one, increasing the number of transport events taking place in the simulation.

## 4. Reports of Rapid Transport and Selectivity in Nanopores

### 4.1. Spontaneous Filling and Rapid Transport

Water molecules have been shown to spontaneously enter and remain inside carbon nanotubes greater than 0.81 nm in diameter (or (6, 6)) in MD simulations.<sup>[3,49]</sup> In contrast, narrower carbon nanotubes, such as (5, 5) with a diameter of 0.69 nm, will only partially fill with water molecules,<sup>[56]</sup> or alternate between empty and filled states.<sup>[3]</sup>

Nanotubes also exhibit unusually high water permeation rates in simulation, with water fluxes larger than predicted by continuum hydrodynamics theory.<sup>[2,3,20,49,51–53,55,57–60]</sup> A summary of these results are presented in Table S1 in the Supporting Information. For example, Hummer et al.<sup>[49]</sup> discovered that water permeated a (6, 6) carbon nanotube in burst-like motions, during which water molecules moved with very little resistance. This occurred solely from diffusion of water through the carbon nanotube; a force was not used to drive the process. The average water flux over the course of the simulation was 17 molecules.tube<sup>-1</sup>.ns<sup>-1</sup>, comparable to the flux of a biological counterpart, the aquaporin-1 channel.<sup>[61]</sup>

Experiments by various groups<sup>[1,50]</sup> have also demonstrated unusually large water fluxes. Majumder et al.<sup>[50]</sup> constructed membranes composed of arrays of aligned multi-walled carbon nanotubes with pore diameters of about 7 nm.

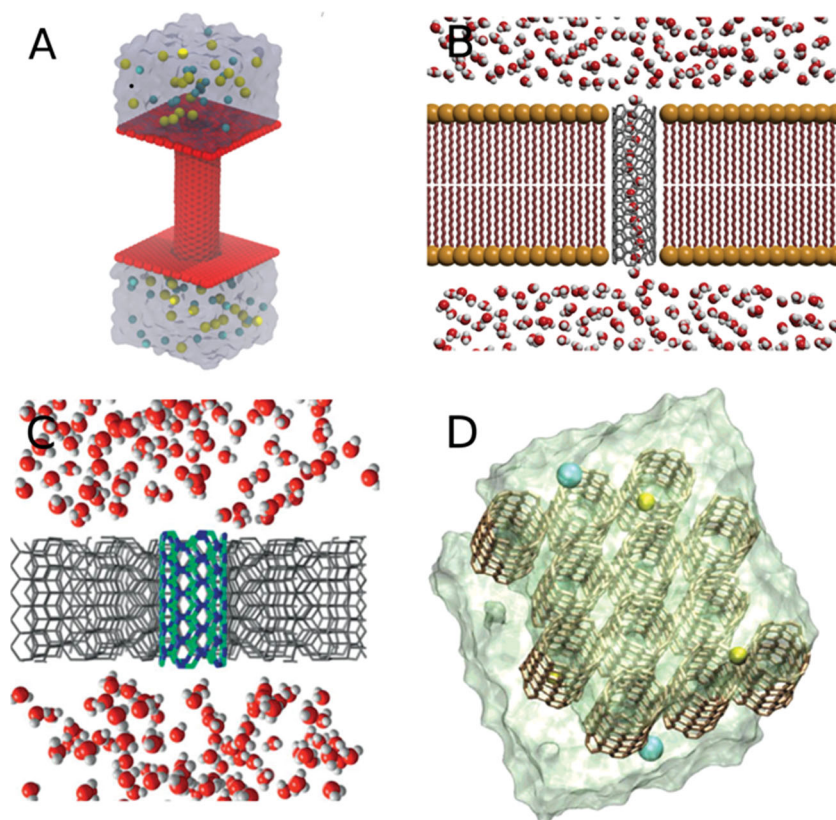


**Figure 2.** Molecular dynamic simulation of nanotubes embedded in various matrices. Images show a nanotube embedded in a (A) graphene bilayer, (B) Lipid bilayer and (C) a Silicon Nitride membrane. (D) An array of nanotubes with no supporting matrix. (B) Reproduced with permission.<sup>[52]</sup> Copyright 2012, American Chemical Society; (C) Reproduced with permission.<sup>[51]</sup> Copyright 2009, Wiley-VCH; (D) Reproduced with permission.<sup>[3]</sup> Copyright 2008, American Chemical Society.

Water flow rates through this membrane were found to be similar to the aquaporin-1, and many orders of magnitude larger than suggested by the Hagen-Poiseuille equation, a conventional continuum flow model. Similarly, Holt *et al.*<sup>[1]</sup> demonstrated that these amazing rapid transport properties occur in narrower nanotubes using membranes composed of 1.3–2.0 nm diameter carbon nanotubes. Water flow rates were three orders of magnitude larger than predicted by a continuum model and were consistent with the rates predicted from MD simulations. The slip length of these nanotubes was found to be incredibly large, indicating that fluid flow is not affected by the liquid/wall interface. Nanotubes have also been dispersed in polymer membranes, where they are able to be partly aligned.<sup>[62,63]</sup> Initial experiments showed rapid gas flow across these membranes,<sup>[62]</sup> and recently it has been shown both computationally and experimentally that zwitterion functionalised CNTs can increase the water permeability of the membrane.<sup>[63]</sup> Addition of these zwitterion functionalised CNTs into the polyamide membrane increased both water flux and salt rejection ratio, confirming that the water molecules were traversing through the CNT interior. These experimental results indicated that the interior of the both large and narrow diameter nanotubes offered a near-frictionless surface for the water molecule to flow across. Although the degree of flow enhancement is not consistent amongst all

these studies, it has been suggested that this can be explained by accounting for the specific water-pore interactions found in each case.<sup>[64]</sup>

Typically carbon nanotubes are modelled in MD simulations with a zero partial charge on each carbon atom. In contrast, boron nitride nanotubes and silicon nitride nanotubes have differing partial charges on each boron and nitrogen, and silicon and carbon atoms respectively. These charges, combined with the van der Waals parameters, allow water molecules to hydrogen bond with the nitrogen or carbon atoms respectively.<sup>[31]</sup> As such, boron nitride nanotubes spontaneously fill at smaller pore diameters than carbon nanotubes in simulation studies, owing to the increased van der Waals and electrostatic interactions between the water molecules and nanotube atoms.<sup>[31,51,56]</sup> It is likely that the filling of silicon carbide nanotubes is similar to that in boron nitride nanotubes.<sup>[32,65]</sup>

Nanoporous graphene has recently attracted attention for its potential to provide an even larger throughput of water than nanotube based membranes.<sup>[66–68]</sup> Using MD simulations, Suk and Aluru<sup>[68]</sup> demonstrated that for large diameter pores, where single-file water transport is not observed, water flux is higher than through a carbon nanotube membrane of similar diameter. On the other hand,

for smaller diameter nanoporous graphene in which single-file transport is observed, water flux is lower than in carbon nanotube membranes. Cohen-Tanugi and Grossman<sup>[67]</sup> demonstrate that nanoporous graphene has water permeability several orders of magnitude higher than conventional reverse osmosis membranes. Moreover, by functionalizing the nanopores with either hydroxyl groups or hydrogen atoms they demonstrate the ability to reject salt ions. Konatham *et al.* also demonstrate the ability to reject salt ions with graphene nanopores functionalized with carboxyl groups.<sup>[69]</sup>

#### 4.2. Ion Rejection

It was quickly recognised that if the rapid transport properties of nanotubes could be coupled with the rejection of salts and other water contaminants, there could be potential applications of these pores in water purification. A number of experimental and simulations studies have therefore investigated this. MD simulations have demonstrated that nanotubes below a certain radius are able to reject ions whilst maintaining large water fluxes.<sup>[3,59,60,70]</sup> For example, Corry<sup>[3]</sup> quantitatively determined the salt rejection of (5, 5), (6, 6), (7, 7) and (8, 8) (0.66, 0.81, 0.93, 1.09 nm diameter, respectively) carbon nanotubes under a hydrostatic pressure of 208 MPa

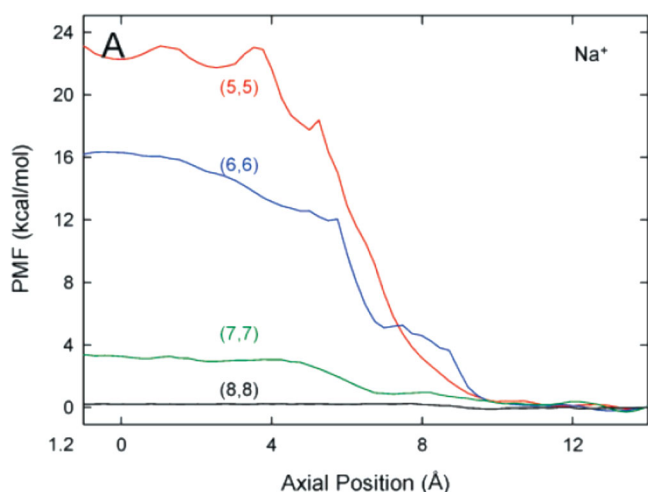


**Figure 3.** The free energy profile of  $\text{Na}^+$  permeating through carbon nanotubes of various pore diameters. The left hand side of the graph is the centre of the nanotube and the right hand side is bulk water. Reproduced with permission.<sup>[3]</sup> Copyright 2008, American Chemical Society.

to be 100%, 100%, 95% and 58%. Investigations have identified a large free energy barrier for  $\text{Na}^+$  ions to permeate across (6, 6) carbon nanotubes but a relatively small barrier for the larger (8, 8) or (10, 10) nanotubes,<sup>[3,60,70]</sup> as illustrated in **Figure 3**.

Ion rejection by nanotubes has also been demonstrated experimentally.<sup>[71]</sup> Nanotubes with pore diameters 1–2 nm were shown to partially reject a number of salts, including  $\text{Na}^+$  and  $\text{Cl}^-$ , with rejection reaching 98% under certain conditions. In this study chemical etching was used to remove the nanotube caps, resulting in functionalized ends with carboxylic, carbonyl and hydroxyl groups. Ion rejection was found to be dependent on pH, and the rejection rate was found to decrease as the concentration of the salt increased. As discussed later, this rejection appears to originate from a different mechanism to that seen in simulations.

Alternative nanotube materials have also demonstrated the ability to reject salt in MD simulations.<sup>[51,52]</sup> In one study hydrostatic pressure was used to force a NaCl solution through a single boron nitride nanotube embedded in a silicon nitride membrane.<sup>[51]</sup> The 0.69 nm diameter, (5, 5) boron nitride nanotubes completely rejected both  $\text{Na}^+$  and  $\text{Cl}^-$  ions. In contrast, the salt rejection properties are reversed in the 1.1 nm (8, 8) nanotubes;  $\text{Na}^+$  is completely rejected, while  $\text{Cl}^-$  is able to pass. Similarly, a 0.86 nm diameter, (5, 5) silicon carbide nanotube completely rejected both  $\text{Na}^+$  and  $\text{Cl}^-$ , much like its boron nitride counterpart.<sup>[52]</sup> In addition, much like boron nitride nanotubes, the rejection properties of  $\text{Na}^+$  and  $\text{Cl}^-$  are reversed when the radius increases to 1.0 nm and 1.2 nm;  $\text{Cl}^-$  is able to permeate the pores, while  $\text{Na}^+$  is rejected.<sup>[52]</sup>

Functionalization can also affect the permeation and rejection properties of nanotubes.<sup>[58,72]</sup> Corry<sup>[58]</sup> functionalize 1.1 nm diameter, (8, 8) carbon nanotubes with varying numbers (either 2, 4 or 8) of  $\text{COO}^-$ ,  $\text{NH}_3^+$ , OH and  $\text{CONH}_2$  functional groups, as well as a mixtures of  $\text{NH}_4^+$  and  $\text{COO}^-$ , at the upstream pore opening (as shown in **Figure 4**). Higher salt rejection was achieved in these functionalized pores than

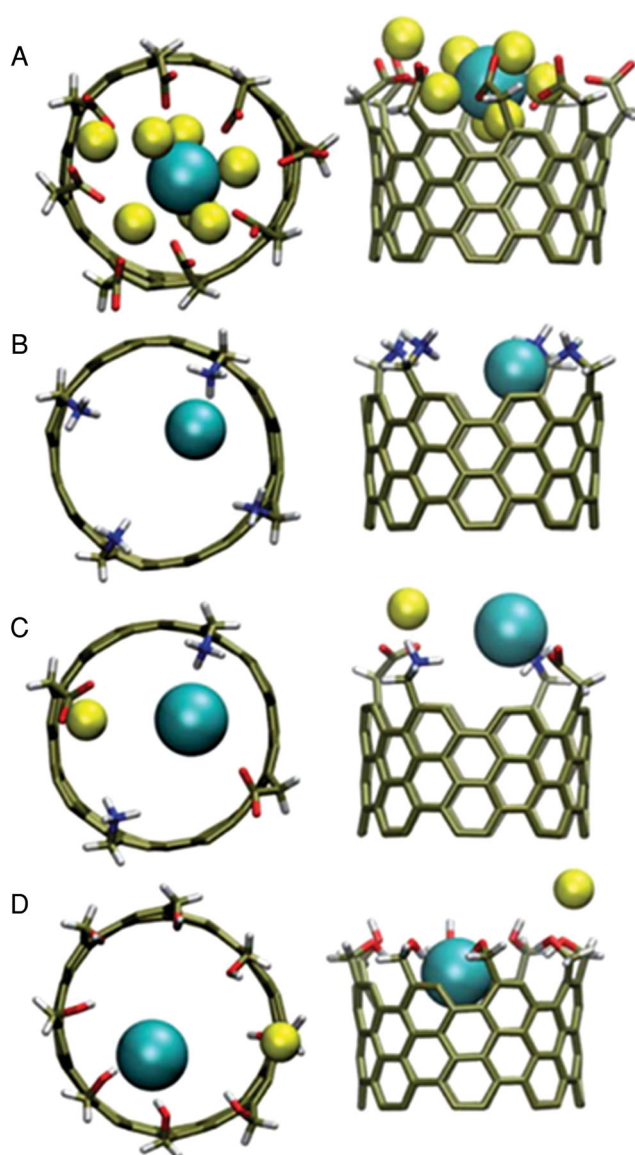


**Figure 4.** Top (left) and side (right) views of the position of ions near the pore opening of functionalised carbon nanotubes. Sodium ions are represented by yellow, chloride ions by cyan, carbon by beige, oxygen by red, nitrogen by blue and hydrogen by white. The carbon nanotubes depicted here are functionalised with (A)  $8\text{COO}^-$ , (B)  $4\text{NH}_4^+$ , (C)  $2\text{COO}^-$  and  $2\text{NH}_4^+$  and (D)  $8\text{OH}$ . Reproduced with permission.<sup>[58]</sup> The Royal Society of Chemistry.

in pristine nanotubes, for example 100% rejection of  $\text{Na}^+$  and  $\text{Cl}^-$  ions was obtained for the  $8\text{COO}^-$ ,  $4\text{NH}_4^+$  and  $3 \times 4\text{NH}_4^+$  groups. However, the most marked difference between the pristine and functionalised carbon nanotubes was the reduction in the water flux for all tested functionalised nanotubes, ranging from 67% to 13% of the pristine carbon nanotube flux. The mechanism behind this reduction is discussed in section 5.2. MD simulations of narrow graphene pores have shown that salt rejection depends critically upon the pore size and chemical nature.<sup>[67]</sup> Near complete rejection was seen with hydrogenated pores, but increasing the polarity of the pore rim with hydroxyl groups reduced salt rejection except in very narrow pores.

### 4.3. Selection Between Ions

Ion selectivity can be defined as a significant difference in the ability of a pore to pass/reject two ion types. This ability is very important in various biological processes; the selection between anions and cations is important for the regulation of blood pressure and organelle acidification, while the selection between  $\text{Na}^+$  and  $\text{K}^+$  is important for nerve conduction and maintaining electrochemical gradients across cells.<sup>[73]</sup> Many proteins have developed the ability to discern between these ions, making these processes possible. One particular class of these proteins, called ion channels, are able to distinguish between ion types at near diffusion limited rates.<sup>[74–77]</sup> Nanotubes have the ability to mimic and replicate these properties for use in a range of applications, including ultra sensitive ion detection and antimicrobial agents.

Ion selectivity between cations and anions has been demonstrated in a range of nanotube structures. Song and Corry<sup>[60]</sup> demonstrated  $\text{Na}^+/\text{K}^+$  selectivity in pristine carbon nanotubes, the free energy barrier was larger for  $\text{K}^+$  in (5, 5) and (6, 6) carbon nanotubes, for  $\text{Na}^+$  in (7, 7) and (8, 8) nanotubes and roughly equal in (9, 9) nanotubes. Similar principles have been shown for selection between anions in simplified narrow pores.<sup>[78,79]</sup> Moreover, (9, 9) carbon nanotubes functionalized with carbonyl groups at the pore openings are selective for  $\text{Cl}^-$  over  $\text{Na}^+$ ,<sup>[80]</sup> and display similar conductance properties as biological  $\text{Cl}^-$  selective ion channels, such as  $\text{Cl}^-$  channels and GABA receptors. As well as the ability to selectively conduct  $\text{Cl}^-$  ions these nanotubes also exhibit ion conductance significantly larger than their biological counterparts,<sup>[80]</sup> and this has also been observed in other nanotubes.<sup>[81]</sup> Alternative nanotube materials have also demonstrated selectivity. For example, (6, 6) and (7, 7) boron nitride nanotubes are selective for  $\text{Na}^+$  over  $\text{Cl}^-$ ,<sup>[51]</sup> while (10, 10) boron nitride nanotubes are selective for  $\text{Cl}^-$  over  $\text{K}^+$ , the opposite of the selectivity found in (10, 10) carbon nanotubes.<sup>[82]</sup> Pristine (6, 6) and (7, 7) silicon carbide nanotubes have an intrinsic selectivity for  $\text{Cl}^-$  over  $\text{Na}^+$ .<sup>[52]</sup>

The interior of pores have been targeted as sites of functionalization, rather than the pore openings, in attempt to mimic biological ion selective structures.<sup>[53]</sup> For example, a (9, 9) carbon nanotube functionalized with carbonyl oxygens, shown in **Figure 5**, was found to display selectivity between  $\text{Na}^+$  and  $\text{K}^+$  in MD simulations. Three different configurations of carbonyl groups were studied; each producing marked differences in selectivity. Surprisingly, the configuration mimicking the selectivity filter of a potassium channel (four sets of four carbonyl oxygens arranged in four rings) resulted in a  $\text{Na}^+$  selective nanotube, highlighting the difficulty to predict a priori the selectivity of functionalised nanotubes, given the number of factors involved in determining selectivity.

Sint et al.<sup>[83]</sup> designed graphene nanopores that were selective to cations and anions by functionalizing the nanopore with either nitrogen and fluorine, or hydrogen, respectively. They

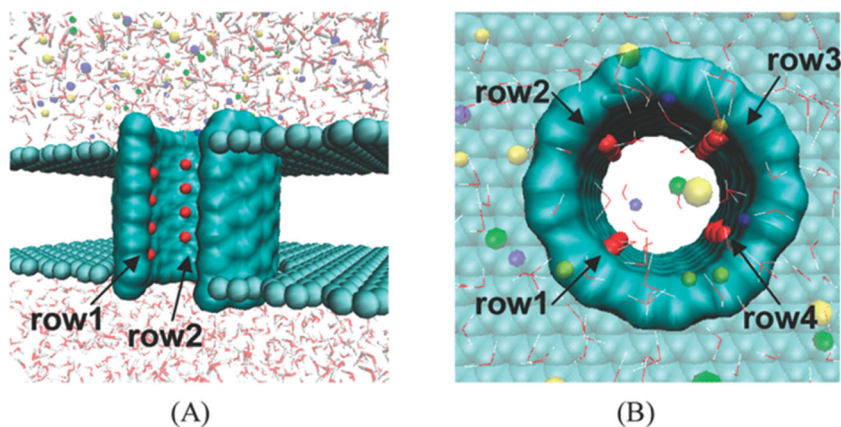


**Figure 5.** (A) A side and (B) top view of a (9, 9) carbon nanotube functionalised with carbonyl (C = O) groups to create  $\text{Na}^+/\text{K}^+$  selectivity. Reproduced with permission.<sup>[53]</sup> Copyright 2010, American Chemical Society.

showed using MD that the fluorine/nitrogen lined pores only allowed lithium, sodium and potassium ions to pass through, whereas the hydrogen lined pores allowed only chloride and bromine to cross. Recent simulation studies have also shown how altering the size of graphene nanopores and the charge surrounding them can be used to generate pores selective for either  $\text{Na}^+$  or  $\text{K}^+$ , and that this can be influenced by external fields.<sup>[84]</sup>

## 5. Mechanisms Involved in Transport/Selectivity

One of the most important reasons for running MD simulations is to investigate the mechanisms responsible for the unusual transport and selectivity properties of nanopores. Here we elucidate what has been learnt about the physical basis of the unusual transport properties seen in these pores.

### 5.1. Spontaneous Filling

While it may seem surprising that water will enter a narrow hydrophobic pore, studies suggest that the confinement of water molecules within a nanotube is thermodynamically favourable, that is to say that the free energy is lower in a filled state than an unfilled state.<sup>[21,85]</sup> However, the driving force differs with the pore diameter:

- filling is entropy driven in the smaller diameter (5, 5) and (6, 6) carbon nanotubes (0.81–1.0 nm) due to the increased translations and rotations of water compared to water molecules in bulk water,
- hydrogen bonds between water molecules in the larger (8, 8) and (9, 9) carbon nanotubes (1.1–1.2 nm) impart favourable enthalpic contributions due to a rigid hydrogen bonding network,
- large translational entropy of water molecules in the 1.4 nm (10, 10) nanotube and larger compared to bulk water induces spontaneous filling.

The splitting of the filling driving force into three domains of pore diameter also represents the structure of water in the

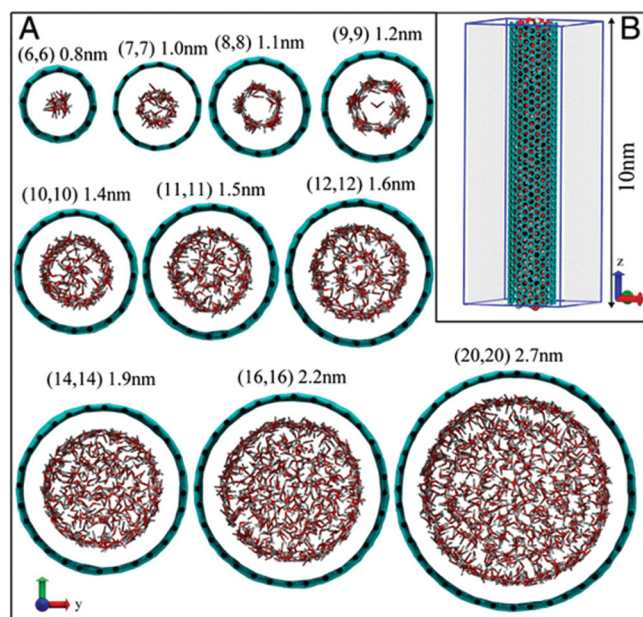


**Figure 6.** The structure of water inside carbon nanotubes of varying diameters. (A) The axial pore distribution looking along the pore axis. (B) A view of the carbon nanotube perpendicular to the pore axis. Reproduced with permission.<sup>[85]</sup> Copyright 2011, National Academy of Sciences.

nanotube in each case.<sup>[85,86]</sup> For the smaller pore sizes, the water is restricted to a single file along the pore axis, resulting in a gas-like phase of water molecules. The next largest domain, incorporating the (8, 8) and (9, 9) carbon nanotubes, is described as an ice-like phase where a slightly increased number of hydrogen bonds per water molecule, as compared to bulk water, restricts the water distribution to a torus perpendicular to the pore axis, as shown in **Figure 6**. As the pore diameter increases further, the structure of water in the nanotube becomes more and more liquid-like. Some layering of the water is still present at the interface with the inner nanotube wall, but this dissipates towards the centre of the tube. Although a similar analysis on the driving force of filling in boron nitride and silicon carbide nanotubes has not been conducted, similar water structures have been observed<sup>[31,65]</sup> and it is assumed that similar processes are at play, although the domains of entropy and enthalpic domination may differ.

## 5.2. Rapid Transport

By following the motion of individual atoms over time, MD simulations have the potential to help us understand the reasons for the rapid transport in CNTs and hydrophobic nanopores. In general, the rapid flow is attributed to a lack of friction between water molecules and the pore walls. In macroscopic models of fluids flowing through a pipe or pore, the velocity of water flow through the pipe is at a minimum at the walls of the pipe due to friction along the wall and at a maximum at the centre of the pipe (similar to the red or blue lines in **Figure 7**).

However in pristine carbon nanotubes, the flow velocity does not dip near the pore walls as shown by the black line

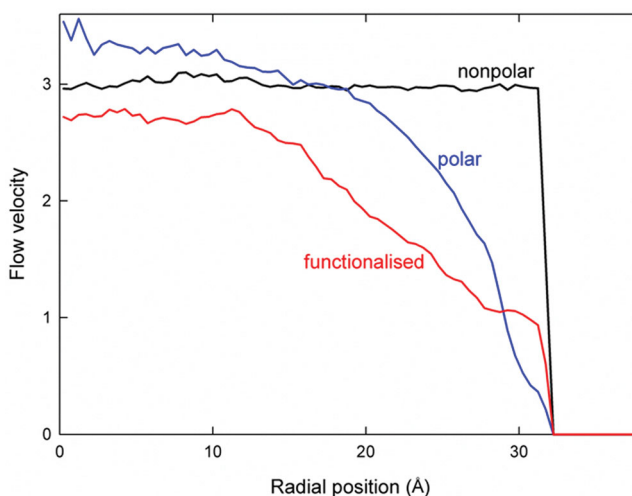


**Figure 7.** The axial velocity profile of water through (50, 50) carbon nanotubes. A pristine, uncharged carbon nanotube is plotted in black (non-polar), a pristine, partially charged carbon nanotube in blue (polar) and a nanotube with bulky, negatively charged functional groups attached along the length of the pore in red. The centre of the pore is at 0 Å and the radius of the carbon nanotube is at 35 Å. Adapted with permission.<sup>[2]</sup> Copyright 2011, The Royal Society of Chemistry.

in **Figure 7**, indicative of very little friction.<sup>[2]</sup> Similar profiles are expected for varying diameter and length nanotubes. The near frictionless flow of water through the nanotube implies that the water flux across any plane perpendicular to the pore axis is independent of the length of the tube, which has been confirmed by various MD simulations studies,<sup>[3,59,87]</sup> although there are some reports counter to this.<sup>[54]</sup> But, despite much discussion, the reason for this lack of friction is still not clear. Simulation studies have suggested a number of reasons for the low friction:

1. The electrically and mechanically smooth walls of the CNT create a frictionless surface.<sup>[2,88–90]</sup>
2. The formation of a vapour or depletion layer on the on the CNT walls.<sup>[49,59,88]</sup>
3. A layer of water on the walls screens the remaining water molecules.<sup>[91]</sup>

Most MD studies investigating water flow through carbon nanotubes assign a zero partial charge to each carbon atom in the nanotube. As a result, there is no electrostatic interaction; only van der Waals interactions occur between the nanotube and the water molecules. The interaction between neutral carbon and water molecules tends to be quite weak. This allows water molecules to adopt particular orientations and hydrogen bonding at the water/nanotube interface, making the surface of the nanotube ‘slippery’ to water molecules,<sup>[88]</sup> and this is the idea behind the electrically smooth walls aiding rapid transport as described in mechanism (1) above. Ho et al.<sup>[92]</sup> demonstrated using flat surfaces that slip is determined by the distribution of water molecules within the contact layer and by the strength of the water-surface interaction. Similarly, nanotubes (carbon nanotubes especially) have very smooth and uniform walls with very few friction causing bumps along their length. In support of the importance of this smoothness, Joseph and Aluru demonstrated

that the water velocity is significantly reduced when the CNT surface is “roughened”.<sup>[88]</sup>

If non-zero partial charges are assigned to each atom in the carbon nanotube, however, stronger electrostatic interactions are possible with passing water molecules. These interactions slow down the rate at which water can flow across the surface thus creating friction,<sup>[2,93]</sup> as can be seen in Figure 7, reminiscent of the profile in macroscopic models. This decrease is due to additional interactions of the water molecules with the wall of the nanotube, introducing friction into the flow of the water molecules and offering one explanation of the lower flux seen in studies of polarised or functionalised nanotubes.<sup>[2,58,72]</sup>

Which of the mechanisms listed above is most likely to be responsible for the limited friction seen by water passing through the nanotubes? Most evidence suggests that (3) is not the cause of rapid transport. In narrow nanotubes, there is no space for a layer of water at the walls as required to shield faster moving water in the pore center, yet large flows are seen. In addition, in larger diameter nanotubes, water molecules have been shown to move through at the same velocity regardless of radial position, as shown in the black curve in Figure 7. Mechanism (1) and (2) can occur simultaneously, and apply to all nanotube diameters. Both mechanism (1) and (2) occur as a result of the strong hydrogen-bonding between water molecules compared to the weak water-wall interaction. The water-wall interaction is weak since non-polar CNTs are uncharged (electrically smooth) and their atomic structure is fairly rigid and does not readily buckle (mechanically smooth) under the conditions typically used to model water flow rates. These differences in water interactions cause water molecules to move away from the non-polar wall and form a vapour or depletion region,<sup>[49,88]</sup> further reducing the water-wall interaction.

What happens when instead water moves through a more polar tube? The situation here is more complicated and there are many disparate simulation results. For example, adding charges to the end of narrow carbon nanotubes has been shown to increase flow rates,<sup>[20,21]</sup> and water fluxes in boron nitride tubes are potentially larger than those displayed by comparable diameter carbon nanotubes.<sup>[31,56]</sup> However, the addition of polar atoms in carbon nanotubes has also been reported to reduce water fluxes,<sup>[2,88,94]</sup> and if the partial charges of boron nitride and silicon carbide nanotubes are further increased, a decline in the water fluxes is observed.<sup>[31,51]</sup> Similarly, the addition of charges via functional groups to carbon nanotubes has been seen to reduce water fluxes.<sup>[2,58,72]</sup>

How do we make sense of this disparate data? Explaining why increasing nanotube polarity can reduce flow is perhaps most straightforward. Increased polarity in nanotubes can influence both mechanisms of reducing friction described above. Not only does this yield stronger interactions of water with the pore walls reducing the electrical smoothness of the pore (mechanism (1)) and meaning water sticks to the walls,<sup>[2,88]</sup> the vapour or depletion layer mentioned in mechanism (2) is reduced for hydrophilic tubes as water is attracted closer to the pore walls.<sup>[88]</sup> In contrast, the increased flow seen in some situations is probably related to a reduction in

the barrier for water to enter the tube from bulk. In some cases water experiences a barrier to enter a prefilled nanotube (although there is some discrepancy in the magnitude of these).<sup>[20,60]</sup> Adding partial charges to atoms on the tube walls, especially those near the channel mouth, can reduce this barrier as illustrated in **Figure 8**. This effect is likely to be most noticeable in narrow pores where a significant barrier can exist, and is also likely to be overwhelmed when large charges are added to the pore which increases friction along the length of the nanotube.

In summary, both mechanisms (1) and (2) offer plausible and non-exclusive explanations as to why the friction experienced by water in nanotubes is so small and why this yields rapid water flow. Increasing the polarity of the tubes does not always have the same effect on water flux. The reason for this can probably be explained by balancing the effect of this polarity change on the barrier for water entering the pore and the friction for moving along the pore length.

As mentioned, large diameter nanoporous graphene has a larger water flux than carbon nanotube membranes. This is due to a reduced energy barrier for water molecules at the entrance to the pores in graphene since the water baths are directly connected as a result of the one-atom thick membrane.<sup>[68]</sup> When the pore size is reduced so that only single-file water transport is observed, the hydrogen bonds are frequently broken and L/D defect-like orientations are observed.<sup>[68]</sup> The inclusion of polar hydroxyl groups to nanoporous graphene increases water permeability across  $\sim 25 \text{ \AA}^2$  and  $\sim 50 \text{ \AA}^2$  pores.<sup>[67]</sup>

### 5.3. Ion Rejection and Selection

Various mechanisms are involved in the selectivity of molecules through nanopores, such as:

1. Size exclusion (bare ion)
2. Dehydration (size exclusion of hydrated ion) and ion coordination numbers.
3. Charge repulsion
4. Subtler effects involving specific interactions with the pore as observed in biological channels
5. The interactions of solutes with specific chemical structures of the pore
6. Entropic differences

The simplest mechanism is size-exclusion. If the size of the ion is physically larger than the pore it will not be able to enter due to steric hindrance. However, pore size can also have a subtler effect if we consider that the strong interaction between ions and water molecules means that the ions like to be surrounded by a hydration shell. A ‘softer’ version of size exclusion arises if we consider the size of these solvated ions. In wider nanotubes, ions are able to pass with the full complement of water molecules in their solvation shell. But, once the size of the pore becomes smaller than the size of the solvation shell there is insufficient space for the solvated ion to pass. In this case, some water molecules must be removed from the solvation shell for the ion to fit inside the nanotube and there is an energetic cost to do this, as illustrated

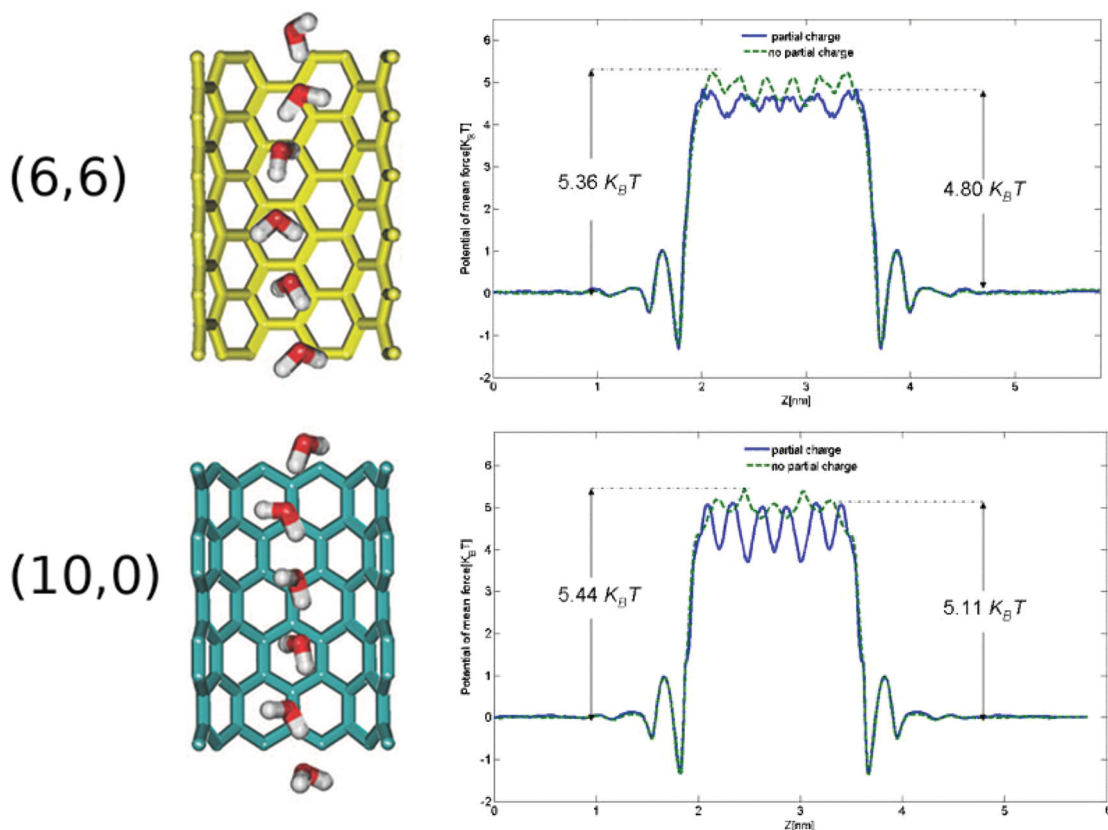


**Figure 8.** The free energy surface for a water molecule to permeate through partially charged (blue line) and uncharged (green line) (6,6) and (10,0) carbon nanotubes. Adapted with permission.<sup>[20]</sup> Copyright 2006, AIP Publishing LLC.

in Figure 3. This makes it far less likely for strongly hydrated ions to permeate narrow tubes.

Ion rejection rates become larger as the nanotube becomes narrower due to the need to remove more water molecules from the ion (**Figure 9**) which comes at increasing cost. The number of water molecules in this solvation shell is termed coordination number for that ion. As illustrated in **Figure 10**, a  $\text{Na}^+$  ion has a coordination number of about 6 in bulk water, but this must reduce to 2 inside a (5, 5), 0.66 nm diameter carbon nanotube.<sup>[3]</sup> As the pore diameter increases, fewer water molecules are required to be removed from the solvation shell for the ion to move through the nanotube. At a diameter of 1.09 nm (an (8, 8) carbon nanotube) the coordination number inside the tube is similar to that in bulk water and there is little cost for this ion to move through the pore. A similar observation is made in MD studies of nanoporous graphene.<sup>[69]</sup>

The differences in how strongly each ion holds its surrounding water (quantified by the free energy of hydration) and the size of each hydrated ion dictates the selectivity sequence of a given pore, and this sequence will often change as a function of pore radius.<sup>[60,78,79,95]</sup> Narrow pores tend

to have the greatest rejection for small highly charged ions as they hold the surrounding water most strongly. The small ions often fit in wider pores with a full solvation shell, and so there is a greater rejection for the larger ions that have to have some water molecules removed from them. Similar principles of differing hydration energies for different species can also explain why water can pass through pristine narrow carbon nanotubes but ions cannot. Although water also interacts with surrounding water molecules, the strength of these interactions is much less than for charged ions. Thus the penalty

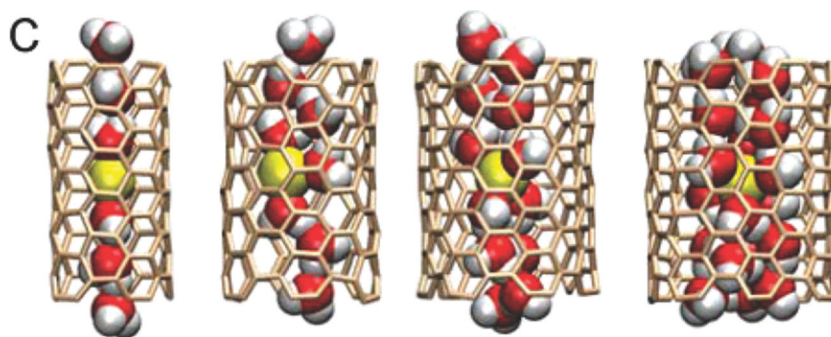


**Figure 9.** In narrow nanotubes (left) very few water molecules coordinate with a permeating ion (sodium in yellow). In wider nanotubes (right), water coordination is more bulk like, resulting in a smaller energy barrier for ion conduction. Oxygen is represented in red, hydrogen in white and carbon in brown. Reproduced with permission.<sup>[3]</sup> Copyright 2008, American Chemical Society.

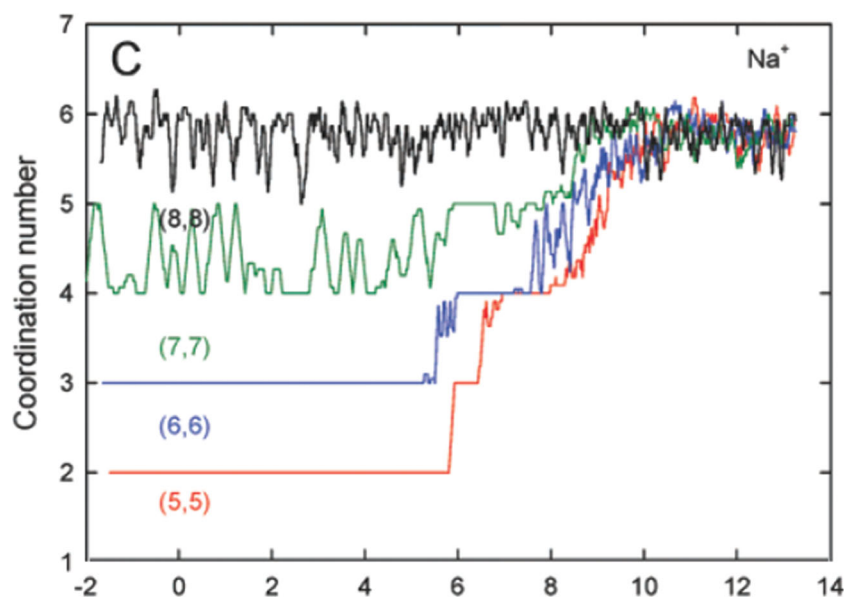


**Figure 10.** The coordination number of a  $\text{Na}^+$  ion as it moves from carbon nanotubes of various diameter pores (left hand side of graph) to bulk water (right hand side of graph). Reproduced with permission.<sup>[3]</sup> Copyright 2008, American Chemical Society.

for removing the surrounding water molecules as required to enter a narrow pore is much less for water than it is for ions.<sup>[3]</sup>

The mechanism of ion rejection in most MD studies of pristine nanotubes differs from that in the current experimental investigations of nanotubes. The former focuses on narrow nanotubes, usually with pore diameters about 1 nm or less, whereas the latter investigates nanotubes with pores wider than 1 nm. Ions need to dehydrate to enter narrow tubes; thus a size-exclusion mechanism is operating on hydrated or bare ions. Ion rejection in wider nanotubes is caused by electrostatic interactions between ions and functional groups at the nanotube pore opening. For example, the experimental work of Fornasiero et al.<sup>[71]</sup> used nanotubes with functional groups at their pore opening and determined that salt rejection is dependent on a number of factors including solution pH and the valency of the ions. These factors indicate that rejection of the ions is occurring via electrostatic interactions between the carbon nanotube pore opening or membrane surface and the ions, rather than steric hindrance at the nanotube opening.

The addition of functional groups at the pore entrance has also been shown to affect the ion rejection and selectivity of narrow nanotubes in MD studies. The situation is complicated by factors such as the pore diameter and the flexibility of the functional groups. For example,  $\text{Cl}^-$  rejection will increase if narrow nanotubes are functionalised with  $\text{COO}^-$  groups due to electrostatic repulsion. However, in wider nanotubes  $\text{Na}^+$  will aggregate around these  $\text{COO}^-$  groups, shielding the negative charge of the functional groups, allowing  $\text{Cl}^-$  to pass through the nanotube as illustrated in Figure 4A.

## 6. Modeling Limitations

The use of MD involves many approximations that have the potential to compromise simulation results if not carefully

considered. MD does not have the ability to model bond formation or destruction as electrons are not modelled explicitly, as in quantum mechanical simulations. This means that MD is unable to capture any chemistry that may take place. This may be of particular importance when considering possible bond formation during chemical fouling of desalination membranes, or the role that functional groups attached to the end of nanotubes may play in water/ion flow rates. More fundamentally, the forces between atoms are calculated using an empirical force field, a set of functions that has to be carefully parameterised. The outcome will only be as good as the choice of function and parameters. Moreover, force field parameters in MD only describe the average properties of a large number of a particular type of molecules, and so in conditions or environments that stray significantly from this, inaccurate results are likely to be produced. For instance, non-polarisable force fields are

unable to handle polarisation explicitly, instead polarisation is accounted for in an average sense by being incorporated into other parameters. Recent long timescale MD simulations have indicated that further work is required to improve current force fields.<sup>[96]</sup>

In order to interpret the MD studies it is important to know how accurately they can reproduce experimental data. It has been shown that hydration and flow in narrow CNTs is extremely sensitive to subtle changes in force field parameters.<sup>[49]</sup> Our own investigations have shown that predicted fluxes can also be sensitive to simulation protocols, such as the mechanisms used for creating hydrostatic pressure and maintaining temperature. However, analysis over many MD studies with different simulation parameters agree that fast transport is indeed occurring and several orders of magnitude larger than predictions from continuum theory. Ion rejection, in its various forms, is also seen to occur in many situations across a range of simulation conditions.

Finally, it is hard to assess the limitations of MD simulations since at present experimental work confirming simulation results is lacking. This is largely due to the fact that simulations focus on a small number of narrow, chemically simple nanotubes; while experiment is usually done on a large number of wider, more disparate and poorly characterised tubes. Further work is necessary to provide a direct link between these two approaches. Currently, MD is beneficial as a means to investigate mechanisms and guide experimenters working in the area.

## 7. Applications

The water and ion permeation properties of nanotubes make them ideal for use in many types of applications. The feasibility of using carbon nanotubes as efficient water purification

devices<sup>[1,71]</sup> or single-ion detectors<sup>[10]</sup> has been demonstrated experimentally. Computational modelling helps to guide the design of, and provide predictions for, potential applications.

Using nanotube-based reverse osmosis membranes for seawater desalination has attracted enormous attention. MD simulations have demonstrated that some nanotubes have greatly increased water fluxes compared to commercially available membranes, while being able to maintain the necessary 95% salt rejection that is required for potable water. However, there are two issues that may limit the implementation of this technology, firstly the inability to fabricate a very narrow distribution of nanotube diameters and secondly, the cost of implementation of nanotube-based RO membranes currently outweighs the cost of purchasing and installing more traditional membrane modules. A possible advantage of having a high flux nanotube membrane could lie in reducing the size of the desalination plant, which may find specialised applications in places where size and weight are limited, e.g. space missions. Nanoporous graphene has also been proposed for desalination membranes as it may help to overcome some of the issues associated with nanotube membranes.<sup>[66,67]</sup>

Nanotube based membranes may still prove to be more resistant to fouling, a common problem in currently used membranes. A number of organic and inorganic species are able to physically and chemically occlude pores, and therefore membranes must be regularly cleaned. Carbon nanotubes have been demonstrated to be able to be readily functionalised; perhaps the more chemically inert boron nitride and silicon nitride nanotubes will be more resistant to fouling. More research is required to determine the ability of these nanotubes to resist fouling. MD is not able to simulate chemical reactions taking place during chemical fouling of the membrane. There are other computational techniques that are available to study this such as quantum mechanical and hybrid quantum mechanical/molecular dynamic techniques. However, fouling in the form of physical blockage could potentially be modelled by MD for small fouling species.

The recycling of wastewater is becoming more popular as traditional water sources become scarcer. Filtration techniques employed by water treatment facilities allow some potentially harmful molecules such as endocrine disrupting chemicals to pass through.<sup>[97]</sup> In addition, it has been determined that traditional nanofiltration membranes allow the passage of hormones such as testosterone and progesterone.<sup>[98]</sup> The removal of heavy metals from water is also vital for the success of water recycling, and nanofiltration membranes may aid this goal. The selectivity properties of nanotube based membranes make them ideal candidates as filtration membranes. The more rigid structure of nanotubes than polymers can allow for high levels of selectivity which may be useful for filtering of these species. Moreover, since nanotubes are more well-defined than polymer membranes they provide a model system for the study of the mechanisms which are occurring in other systems.

Ion-selective nanopores could also lead to practical nanodevices in biomedical applications, such as antimicrobial agents, nanofluidic devices and biosensors. An ion-selective nanopore which is able to embed within a lipid bilayer<sup>[99]</sup>

and mimic the function of a biological ion channel may lead to the design of new pharmaceutical products. For example, Hilder and Chung<sup>[81]</sup> designed a carbon nanotube with the ability to mimic the function of the antibiotic gramicidin-A, but with much larger ionic conduction. Gramicidin-A was one of the first antibiotics isolated and used clinically, and acts by selectively conducting monovalent cations across the bacterial cell membrane, thus rendering the bacteria unviable. Ion-selective nanopores with enhanced ionic conduction could also be utilized as ultra-sensitive biosensors. Hilder and colleagues<sup>[11]</sup> have also designed a biosensor concept, based on a similar principle to the ICS<sup>TM</sup> biosensor,<sup>[100]</sup> comprised of an array of functionalized carbon nanotubes and fluorinated fullerenes. This design has a number of possible advantages over the ICS<sup>TM</sup> biosensor including a 20-fold increase in ionic conductance, the potential to activate a large number of channels since the nanotubes can be densely packed into a membrane, and the potential to be a more sensitive current amplifier since current can be measured directly.

## 8. Conclusion

Molecular dynamics is a computer simulation technique that provides a powerful tool to investigate the transport and selectivity of various nanopores as it allows for the motions of individual atoms to be described. This review highlights some of the unusual transport and selectivity properties of nanotubes, and nanoporous graphene that have been observed in MD simulations such as spontaneous filling by water, high water throughputs, salt rejection and ion selectivity. In addition we have aimed to clarify the physical mechanisms that create these remarkable properties. While we believe that a better understanding of the transport and selectivity in nanopores will aid in the design of novel technological devices, we note that there is still a large gap in nanoporous systems being studied with experimental and simulation approaches which has made it hard to verify the results of the simulation work. We hope that a closer union of simulation and experiment will advance this field further in the future.

## Supporting Information

Supporting Information is available from the Wiley Online Library or from the author.

- [1] J. K. Holt, H. G. Park, Y. M. Wang, M. Stadermann, A. B. Artyukhin, C. P. Grigoropoulos, A. Noy, O. Bakajin, *Science* **2006**, *312*, 1034–1037.
- [2] M. Majumder, B. Corry, *Chem. Commun.* **2011**, *47*, 7683–7685.
- [3] B. Corry, *J. Phys. Chem. B* **2008**, *112*, 1427–1434.
- [4] S. A. Kosa, G. Al-Zhrani, M. A. Salam, *Chem. Engin. J.* **2012**, *181–182*, 159–168.
- [5] M. A. Salam, *Int. J. Environmental Sci. Technol.* **2013**, *10*, 677–688.

- [6] J. Lee, N. R. Aluru, *J. Membrane Sci.* **2013**, *428*, 546–553.
- [7] J. H. Park, S. B. Sinnott, N. R. Aluru, *Nanotechnology* **2006**, *17*, 895–900.
- [8] X. Diao, H. Chen, G. Zhang, F. Zhang, X. Fan, *J. Nanomaterials* **2012**, *2012*, 806019.
- [9] N. Ashkenasy, J. Sánchez-Quesada, H. Bayley, R. Ghadiri, *Angew. Chem.* **2005**, *117*, 1425–1428.
- [10] C. Y. Lee, W. Choi, J. H. Han, M. S. Strano, *Science* **2010**, *329*, 1320–1324.
- [11] T. A. Hilder, R. J. Pace, S. H. Chung, *Sensors* **2012**, *12*, 13720–13735.
- [12] P. Abgrall, N. T. Nguyen, *Anal. Chem.* **2008**, *80*, 2326–2341.
- [13] E. A. Müller, *Curr. Opin. Chem. Engin.* **2013**, *2*, 223–228.
- [14] H. Ebro, Y. M. Kim, J. H. Kim, *J. Membr. Sci.* **2013**, *438*, 112–125.
- [15] T. A. Hilder, D. Gordon, S. H. Chung, *Nanomedicine-Nanotechnol. Biol. Medicine* **2011**, *7*, 702–709.
- [16] L. Guan, K. Suenaga, S. Iijima, *Nano Lett.* **2008**, *8*, 459–462.
- [17] J. Yan, L. F. Yi, W. R. Zhong, *J. Serb. Chem. Soc.* **2005**, *70*, 277–282.
- [18] B. J. Hinds, N. Chopra, T. Rantell, R. Andrews, V. Gavalas, L. G. Bachas, *Science* **2004**, *303*, 62–65.
- [19] J. K. Holt, A. Noy, T. Huser, D. Eaglesham, O. Bakajin, *Nano Lett.* **2004**, *4*, 2245–2250.
- [20] C. Y. Won, S. Joseph, N. R. Aluru, *J. Chem. Phys.* **2006**, *125*, 114701.
- [21] D. Y. Lu, Y. Li, S. V. Rotkin, U. Ravaioli, K. Schulten, *Nano Lett.* **2004**, *4*, 2383–2387.
- [22] Y. Fan, B. R. Goldsmith, P. G. Collins, *Nat. Mater.* **2005**, *4*, 906–911.
- [23] L. Duclaux, *Carbon* **2002**, *40*, 1751–1764.
- [24] I. O. Maciel, J. Campos-Delgado, E. Cruz-Silva, M. A. Pimenta, B. G. Sumpter, V. Meunier, F. López-Urías, E. Muñoz-Sandoval, H. Terrones, M. Terrones, A. Jorio, *Nano Lett.* **2009**, *9*, 2267–2272.
- [25] K. Balasubramanian, M. Burghard, *Small* **2005**, *1*, 180–192.
- [26] P. Fortina, L. J. Kricka, S. Surrey, P. Grodzinski, *Trends Biotechnol.* **2005**, *23*, 168–173.
- [27] N. G. Chopra, R. J. Luyken, K. Cherry, V. H. Crespi, M. L. Cohen, S. G. Louie, A. Zettl, *Science* **1995**, *269*, 966–967.
- [28] C. Pham-Huu, N. Keller, G. Ehret, M. J. Ledoux, *J. Catalysis* **2001**, *200*, 400–410.
- [29] X. H. Sun, C. P. Li, W. K. Wong, N. B. Wong, C. S. Lee, S. T. Lee, B. K. Teo, *J. Amer. Chem. Soc.* **2002**, *124*, 14464–14471.
- [30] A. Mavrandonakis, G. E. Froudakis, M. Schnell, M. Mühlhäuser, *Nano Lett.* **2003**, *3*, 1481–1484.
- [31] C. Y. Won, N. R. Aluru, *J. Phys. Chem. C* **2008**, *112*, 1812–1818.
- [32] R. Yang, T. A. Hilder, S. H. Chung, A. Rendell, *J. Phys. Chem. C* **2011**, *115*, 17255–17264.
- [33] K. M. Alam, A. K. Ray, *Nanotechnology* **2007**, *18*, 495706.
- [34] K. M. Alam, A. K. Ray, *Phys. Rev. B* **2008**, *77*, 035436.
- [35] N. Park, J. Cho, H. Nakamura, *J. Phys. Soc. Jpn.* **2004**, *73*, 2469–2472.
- [36] E. T. Thostenson, Z. F. Ren, T. W. Chou, *Composites Sci. Technol.* **2001**, *61*, 1899–1912.
- [37] S. C. O'Hern, C. A. Stewart, M. S. H. Boutilier, J. C. Idrobo, S. Bhaviripudi, S. K. Das, J. Kong, T. Laoui, M. Atieh, R. Karnik, *ACS Nano* **2012**, *6*, 10130–10138.
- [38] J. S. Bunch, Y. Yaish, M. Brink, K. Bolotin, P. L. McEuen, *Nano Lett.* **2005**, *5*, 287.
- [39] R. M. Westervelt, *Science* **2008**, *320*, 324–325.
- [40] A. Dimiev, *Science* **2011**, *332*, 306–306.
- [41] Q. H. Wang, M. C. Hersam, *MRS Bull.* **2011**, *36*, 532–542.
- [42] I. S. Byun, D. Yoon, J. S. Choi, I. Hwang, D. H. Lee, M. J. Lee, T. Kawai, Y. W. Son, Q. Jia, H. Cheong, B. H. Park, *ACS Nano* **2011**, *5*, 6417–6424.
- [43] D. C. Bell, M. C. Lemme, L. A. Stern, J. Williams, C. M. Marcus, *Nanotechnology* **2009**, *20*, 455301.
- [44] D. E. Lobo, J. Fu, T. Gengenbach, M. Majumder, *Langmuir* **2012**, *28*, 14815–14821.
- [45] C. J. Russo, J. A. Golovchenko, *Proc. Natl. Acad. Sci. USA* **2012**, *109*, 5953–5957.
- [46] A. Striolo, A. A. Chialvo, K. E. Gubbins, P. T. Cummings, *J. Chem. Phys.* **2005**, *122*, 234712.
- [47] A. Striolo, A. A. Chialvo, P. T. Cummings, K. E. Gubbins, *J. Chem. Phys.* **2006**, *124*, 074710.
- [48] A. Striolo, A. A. Chialvo, P. T. Cummings, K. E. Gubbins, *Langmuir* **2003**, *19*, 8583–8591.
- [49] G. Hummer, J. C. Rasaiah, J. P. Noworyta, *Nature* **2001**, *414*, 188–190.
- [50] M. Majumder, N. Chopra, R. Andrews, B. J. Hinds, *Nature* **2005**, *438*, 930–930.
- [51] T. A. Hilder, D. Gordon, S. H. Chung, *Small* **2009**, *5*, 2183–2190.
- [52] T. A. Hilder, R. Yang, D. Gordon, A. P. Rendell, S. H. Chung, *J. Phys. Chem. C* **2012**, *116*, 4465–4470.
- [53] X. J. Gong, J. C. Li, K. Xu, J. F. Wang, H. Yang, *J. Am. Chem. Soc.* **2010**, *132*, 1873–1877.
- [54] J. Y. Su, H. X. Guo, *J. Phys. Chem. B* **2012**, *116*, 5925–5932.
- [55] F. Q. Zhu, K. Schulten, *Biophys. J.* **2003**, *85*, 236–244.
- [56] C. Y. Won, N. R. Aluru, *J. Am. Chem. Soc.* **2007**, *129*, 2748.
- [57] M. E. Suk, A. V. Raghunathan, N. R. Aluru, *Appl. Phys. Lett.* **2008**, *92*, 133120.
- [58] B. Corry, *Energy Environ. Sci.* **2011**, *4*, 751–759.
- [59] A. Kalra, S. Garde, G. Hummer, *Proc. Natl. Acad. Sci. USA* **2003**, *100*, 10175–10180.
- [60] C. Song, B. Corry, *J. Phys. Chem. B* **2009**, *113*, 7642–7649.
- [61] M. L. Zeidel, S. V. Ambudkar, B. L. Smith, P. Agre, *Biochemistry* **1992**, *31*, 7436–7440.
- [62] S. Kim, J. R. Jinschek, H. Chen, D. S. Sholl, E. Marand, *Nano Lett.* **2007**, *7*, 2806–2811.
- [63] W. F. Chan, H. Y. Chen, A. Surapathi, M. G. Taylor, X. Shao, E. Marand, J. K. Johnson, *ACS Nano* **2013**, *7*, 5308–5319.
- [64] D. Mattia, F. Calabrò, *Microfluidics Nanofluidics* **2012**, *13*, 125–130.
- [65] F. Taghavi, S. Javadian, S. M. Hashemianzadeh, *J. Mol. Graph. Model.* **2013**, *44*, 33–43.
- [66] E. N. Wang, R. Karnik, *Nat. Nanotechnol.* **2012**, *7*, 552–554.
- [67] D. Cohen-Tanugi, J. C. Grossman, *Nano Lett.* **2012**, *12*, 3602–3608.
- [68] M. E. Suk, N. R. Aluru, *J. Phys. Chem. Lett.* **2010**, *1*, 1590–1594.
- [69] D. Konatham, J. Yu, T. A. Ho, A. Striolo, *Langmuir* **2013**, *29*, 11884–11897.
- [70] C. Peter, G. Hummer, *Biophys. J.* **2005**, *89*, 2222–2234.
- [71] F. Fornasiero, H. G. Park, J. K. Holt, M. Stadermann, C. P. Grigoropoulos, A. Noy, O. Bakajin, *Proc. Natl. Acad. Sci. USA* **2008**, *105*, 17250–17255.
- [72] Z. E. Hughes, C. J. Shearer, J. Shapter, J. D. Gale, *J. Phys. Chem. C* **2012**, *116*, 24943–24953.
- [73] B. Hille, *Ion Channels of Excitable Membranes* 3rd ed. Sunderland Mass, Sinauer **2001**, *xviii*, from p.814 (8 pages of plates).
- [74] G. Yellen, *J. Gen. Physiol.* **1984**, *84*, 157–186.
- [75] L. Heginbotham, R. Mackinnon, *Biophys. J.* **1993**, *65*, 2089–2096.
- [76] M. LeMasurier, L. Heginbotham, C. Miller, *J. Gen. Physiol.* **2001**, *118*, 303–313.
- [77] C. M. Nimigeon, C. Miller, *J. Gen. Physiol.* **2002**, *120*, 323–335.
- [78] L. A. Richards, A. I. Schafer, B. S. Richards, B. Corry, *Small* **2012**, *8*, 1701–1709.
- [79] L. A. Richards, A. I. Schafer, B. S. Richards, B. Corry, *Phys. Chem. Chem. Phys.* **2012**, *14*, 11633–11638.
- [80] T. A. Hilder, D. Gordon, S. H. Chung, *Biophys. J.* **2010**, *99*, 1734–1742.
- [81] T. A. Hilder, S. H. Chung, *Chem. Phys. Lett.* **2011**, *501*, 423–426.
- [82] C. Y. Won, N. R. Aluru, *Chem. Phys. Lett.* **2009**, *478*, 185–190.
- [83] K. Sint, B. Wang, P. Kral, *J. Am. Chem. Soc.* **2008**, *130*, 16448.

- [84] Z. He, J. Zhou, X. Lu, B. Corry, *ACS Nano* **2013**, *7*, 10148–10157.
- [85] T. A. Pascal, W. A. Goddard, Y. Jung, *Proc. Natl. Acad. Sci. USA* **2011**, *108*, 11794–11798.
- [86] D. I. Keller, S. Acharfi, E. Delacretaz, N. Benammar, M. Rotter, J. P. Pfammatter, V. Fressart, P. Guichenev, M. Chahine, *J. Mol. Cell. Cardiol.* **2003**, *35*, 1513.
- [87] W. D. Nicholls, M. K. Borg, D. A. Lockerby, J. M. Reese, *Microfluidics Nanofluidics* **2012**, *12*, 257–264.
- [88] S. Joseph, N. R. Aluru, *Nano Lett.* **2008**, *8*, 452–458.
- [89] A. Striolo, *Nano Lett.* **2006**, *6*, 633–639.
- [90] J. A. Thomas, A. J. H. McGaughey, *Nano Lett.* **2008**, *8*, 2788–2793.
- [91] E. M. Kotsalis, J. H. Walther, P. Koumoutsakos, *Int. J. Multiphase Flow* **2004**, *30*, 995–1010.
- [92] T. A. Ho, D. V. Papavassiliou, L. L. Lee, A. Striolo, *Proc. Natl. Acad. Sci. USA* **2011**, *108*, 16170–16175.
- [93] L. Hao, J. Su, H. Guo, *J. Phys. Chem. B* **2013**, *117*, 7685–7694.
- [94] A. Striolo, *Nanotechnology* **2007**, *18*, 475704.
- [95] L. A. Richards, B. S. Richards, B. Corry, A. Schaefer, *Environ. Sci. Technol.* **2013**, *47*, 1968–1976.
- [96] M. Jensen, V. Jogini, M. P. Eastwood, D. E. Shaw, *J. Gen. Physiol.* **2013**, *141*, 619–632.
- [97] A. C. Johnson, J. P. Sumpter, *Environ. Sci. Technol.* **2001**, *35*, 4697–4703.
- [98] L. D. Nghiem, A. I. Schäfer, M. Elimelech, *Environ. Sci. Technol.* **2004**, *38*, 1888–1896.
- [99] C. F. Lopez, S. O. Nielsen, P. B. Moore, M. L. Klein, *Proc. Natl. Acad. Sci. USA* **2004**, *101*, 4431–4434.
- [100] B. A. Cornell, V. L. B. Braach-Maksytytis, L. G. King, P. D. J. Osman, B. Raguse, L. Wiczorek, R. J. Pace, *Nature* **1997**, *387*, 580–583.

Received: September 13, 2013  
Revised: November 21, 2013  
Published online: January 25, 2014